

# Microstructural study of aged ferrite powders for sensing layers

Jean-Marc Tulliani<sup>a,\*</sup>, Mirko Borgna<sup>a</sup>, Ivan Grigioni<sup>b</sup>, Isabella Natali Sora<sup>b</sup>

<sup>a</sup>INSTM R.U. PoliTO, Politecnico di Torino, Dipartimento di Scienza Applicata e Tecnologia, Corso Duca degli Abruzzi 24, 10129 Torino, Italy

<sup>b</sup>INSTM R.U. Bergamo and Dipartimento di Ingegneria Industriale, Università di Bergamo, viale Marconi 5, 24044 Dalmine BG, Italy

Received 26 October 2012; accepted 26 November 2012

Available online 3 December 2012

## Abstract

Nanosized powders of  $\text{La}_{0.80}\text{Sr}_{0.20}\text{Fe}_{0.95}\text{Cu}_{0.05}\text{O}_{3-w}$  were investigated in terms of structural, morphological, chemical and surface properties by using several characterization techniques. The XPS and IR measurements showed the presence of surface hydroxide and carbonates species. After calcination of the powders at 900 °C the amount of carbonates decreased but was still significant. The sensing activity of thick film based on  $\text{La}_{0.80}\text{Sr}_{0.20}\text{Fe}_{0.95}\text{Cu}_{0.05}\text{O}_{3-w}$  was tested as a function of relative humidity and the results indicate that (i) after one year of ambient storage the sensing material lost quite completely its sensitivity to humidity, (ii) the sensing activity of the film was mostly re-activated after a thermal treatment at 900 °C for 2 h, and (iii) the huge shift of the detection limit to low RH caused by the presence of 5 mol% Cu is also restored.

© 2012 Elsevier Ltd and Techna Group S.r.l. All rights reserved.

**Keywords:** Lanthanum orthoferrite; Ageing; Nanopowders; Carbonates

## 1. Introduction

Recently, lanthanum strontium copper orthoferrites (LSFC) have been proposed as sensing components in chemical sensors for humidity detection [1]. For the compound  $\text{La}_{0.8}\text{Sr}_{0.2}\text{FeO}_{3-w}$  the sensor response was higher without Cu-addition, but the presence of copper inside the orthoferrite structure causes a huge shift of the sensors response to low relative humidity (RH) values (15% RH for  $\text{La}_{0.8}\text{Sr}_{0.2}\text{Fe}_{0.95}\text{Cu}_{0.05}\text{O}_{3-w}$  compared to 65–70% RH for  $\text{La}_{0.8}\text{Sr}_{0.2}\text{FeO}_{3-w}$ ). Water condensation in the thick-films' mesoporosity proved to govern the sensors' response as these materials are known to behave as *p*-type semiconductors, but their resistance decreased with increasing RH values. Although the LSFC-based humidity sensors showed several promising properties such as a detection limit of 15% RH and a good reproducibility between several measurements, as far as we know their ageing behavior has never been reported. As a part of an ongoing study on  $(\text{La}_{1-x}\text{A}_x)(\text{Fe}_{1-y}\text{B}_y)\text{O}_3$  perovskites [1–4],  $\text{La}_{0.80}\text{Sr}_{0.20}\text{Fe}_{0.95}\text{Cu}_{0.05}\text{O}_{3-w}$  nanopowders were investigated by X-ray photoelectron spectroscopy (XPS) measurements, FTIR

spectroscopy, X-rays powder diffraction, together with sensing activity tests as a function of relative humidity at different ageing times.

## 2. Experimental

### 2.1. Synthesis and physical–chemical characterization of the powders

Lanthanum orthoferrite powders of formula  $\text{La}_{0.80}\text{Sr}_{0.20}\text{Fe}_{0.95}\text{Cu}_{0.05}\text{O}_{3-w}$  (LSFC05) were prepared by citrate auto-combustion of dry gel obtained from a solution of corresponding nitrates in a citric acid solution. The experimental details have been previously reported [2]. The resulting lightweight powder was calcined in air at 600 °C for 3 h to remove any organic residue.

Phase purity, lattice symmetry, and unit-cell parameters were determined by powder X-ray diffraction (XRD). XRD patterns were collected at room temperature (Bruker D8 Advance diffractometer), in the  $2\theta$  range 5–90°, using Cu-K $\alpha$  radiation; the step scan was 0.02°  $2\theta$  and the counting time 10 s per step. The structural refinements were carried out with the Rietveld method of profile analysis. The BET surface area was obtained by nitrogen

\*Corresponding author. Tel.: +39 011 090 4700; fax: +39 011 090 4624.  
E-mail address: [jeanmarc.tulliani@polito.it](mailto:jeanmarc.tulliani@polito.it) (J.-M. Tulliani).

adsorption–desorption isotherms according to the conventional BET method using a Micromeritics ASAP 2010 system. Lanthanum ferrites powders (dispersed in ethanol and ultrasonicated for 1 min in order to break soft agglomerates) were also investigated by means of a laser granulometre (Fritsch Analysette 22) prior to the preparation of the screen-printing inks. The mid-IR ( $500\text{--}3600\text{ cm}^{-1}$ ) spectra were collected with a FTIR system (Tensor 27 Bruker). X-ray photoelectron spectroscopy (XPS) measurements were performed with a 5000 Versa Probe (PHI) using a monochromatic Al  $K_{\alpha}$  X-ray source ( $h\nu = 1486.6\text{ eV}$ ); PHI MultiPak Spectrum software was used to perform curve fitting and to calculate the atomic concentrations.

## 2.2. Sensors' preparation and sensing activity testing

Before the realization of the sensors, the screen-printing ink was prepared as follows: a suitable amount of ethyleneglycol monobutyl ether (Emflow, Emca Remex, USA) in which polyvinyl butyral (Aldrich, USA), acting as the binder, was mixed with 0.5 g of LSFC05 powders. The morphology of the thick films was observed at  $3000\times$  magnification by scanning electron microscopy at 20 kV.

Interdigitated gold electrodes (ESL EUROPE 8835 (520C)) were screen-printed onto  $\alpha\text{-Al}_2\text{O}_3$  planar substrates (Coors Tek, USA, ADS-96R, 96% alumina,  $0.85\text{ cm} \times 5\text{ cm}^2$ ) by using a rubber squeegee and a 270 mesh steel screen; after drying overnight, these devices were heated at  $520^\circ\text{C}$  for 18 min with a  $2^\circ\text{C}/\text{min}$  heating ramp to optimize the electrical conductivity of the electrodes. The ink was then manually screen-printed onto the electrodes and, once dried, the sensors were heat treated at  $900^\circ\text{C}$  for 1 h. The formed films had thicknesses of about  $30\text{--}40\text{ }\mu\text{m}$  and areas of about  $1\text{ cm}^2$ .

The devices were electrically characterized by using a laboratory apparatus, made of a thermostated chamber

working at  $25^\circ\text{C}$  in which RH could be varied from 0% to 96%. These experimental details have been previously reported in Ref. [1]. The sensor response (SR), expressed in %, was defined as the relative variation of the starting resistance, compared with the resistance measured under gas exposure

$$SR = 100|R_0 - R_g|/R_0 \quad (1)$$

where  $R_0$  and  $R_g$  are the starting (in the absence of the test gas) and the gas exposed measured resistances of the sensors, respectively. The sensors were manufactured and immediately tested. Then, they were stored in the laboratory in a non-hermetic box. About 1 year later, their response to humidity was again tested prior and after two successive thermal treatments at  $900^\circ\text{C}$  each of 1 h.

## 3. Results and discussion

The morphology of the LSFC05 nanopowders is shown in Fig. 1a. The BET surface area of LSFC05 was  $21\text{ m}^2/\text{g}$  for the powder calcined at  $600^\circ\text{C}$ , and  $6\text{--}7\text{ m}^2/\text{g}$  after thermal treatment at  $900^\circ\text{C}$ . The surface area values were slightly larger than those reported for undoped  $\text{La}_{0.80}\text{Sr}_{0.20}\text{FeO}_{3-w}$  ( $18\text{ m}^2/\text{g}$  and  $6\text{ m}^2/\text{g}$ ). This trend does reflect the fact that the addition of copper in the orthoferrite causes an increase of the surface area which may be due to the occurrence of a lower temperature during the auto-combustion synthesis, as found for the system  $\text{LaFe}_{1-y}\text{Cu}_y\text{O}_{3-w}$  [3]. The mean crystallite size was calculated from XRD data using the Scherrer equation, and the mean diameter value of LSFC05 agglomerates (particle size) and those corresponding to 10% and 90% of the particle size distributions are reported in Table 1. The XRD data showed that the LSFC05 powders calcined at  $600^\circ\text{C}$  were monophasic, and the unit cell parameters (see Table 1) were in agreement with those previously reported in Ref. [2]. The compound crystallized in the perovskite-like cell of  $\text{LaFeO}_3$  ( $Pnma$  orthorhombic symmetry), and

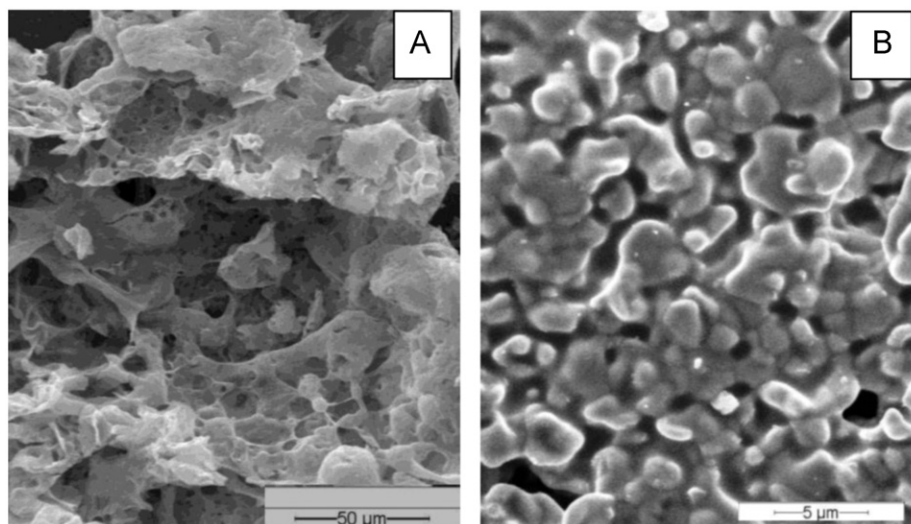


Fig. 1. SEM micrographs of LSFC05: a) powders b) thick film.

with Fe/Cu cations occupying octahedral sites. The unit cell volume decreased with increasing Cu-doping [2]. Since the larger  $\text{Cu}^{2+}$  cation partially substitutes  $\text{Fe}^{3+}$  cation ( $\text{Cu}^{2+}(\text{VI})=0.73 \text{ \AA}$ ,  $\text{Fe}^{3+}(\text{VI})=0.645 \text{ \AA}$ ), a charge compensation mechanism occurs by oxidation of Fe/Cu cations. Preliminary Mössbauer absorption spectra on the isotope  $^{57}\text{Fe}$  carried out at 77 K (not shown) on LSFC05 powders calcined at 900 °C indicated the presence of two sextets with isomer shifts corresponding to  $\text{Fe}^{3+}$  and the presence of one sextet with isomer shift corresponding to  $\text{Fe}^{5+}$ .

XPS measurements were carried out to determine surface composition of aged powders (1 year stored) and after the thermal reactivation treatment in air at 900 °C for 1 h, and to detect chemical species adsorbed on the surface. The XPS survey spectra showed the presence of the expected elements La, Sr, Fe, Cu, O and adventitious carbon, without inorganic contamination. For LSFC05 the O 1s peak shape (Fig. 2) changed significantly as a consequence of the heat treatment at 900 °C. The fitting procedure of the O 1s peaks revealed four contributions: the most intense peak at low binding energies (BEs) (528.3 eV) agrees with the presence of lattice oxygen in the perovskite phase [5,6], and the peak position at 529.3 eV corresponds to the presence of oxygen

bound in simple oxides like  $\text{M}_2\text{O}_3$  or MO. The peaks at higher BEs (530.9 and 532.5 eV) indicated the presence of hydroxide and carbonate species, respectively [5,6]. Two peaks of the C 1s core electrons indicated unambiguously two different states of carbon, one was the signal due to the residual carbon (284.8 eV), and the other contribution at about 289.0 eV corresponded to carbonate species [6]. The carbonate species were not detected by XRD, they are formed mainly on the surface due to exposure to ambient air. After the heat treatment at 900 °C, the intensity of the O 1s peaks at higher BEs (529.6, 531.0 and 532.5 eV) decreased noteworthy. The atomic compositions of the surface samples obtained from XPS analyses indicate that heat treatment causes the decrease of the carbon amount. The surface of the LSFC05 particles is active to chemisorption of  $\text{CO}_2$  in ambient, leading to the formation of carbonate species on the surface. The carbonate species were detected also by FTIR measurements on powders after heat treatment. The IR spectrum of LSFC05 powders heated at 900 °C for 3 h (not shown) showed a broad band in the region 1500–1380  $\text{cm}^{-1}$  associated with the C–O stretchings of surface carbonate species [7,8].

The morphology of the sensing films is shown in Fig. 1b. The thick-films were characterized by a porous glassy-like microstructure and a rather large distribution of agglomerates sizes. Fig. 3 reports the response to humidity of the as manufactured LSFC05 sensor and after about 1 year of storage; in the meantime, the sensing material lost quite completely its sensitivity to humidity. On the contrary, two successive thermal treatments at 900 °C each for 1 h let it to significantly recover its sensing properties.

At room temperature, the resistance–humidity characteristic is mainly determined by the grain surface resistance of the lanthanum ferrite-based materials. In the first stage of water adsorption, a few water vapor molecules tend to chemically adsorb on the grain surfaces of the sample giving rise to La(Sr)-OH hydroxyl groups. Then, physical adsorption of water occurs through hydrogen bonding to the surface hydroxyl groups; this first adsorbed layer is localized by the hydrogen bond of a single water molecule

Table 1

Selected experimental parameters: BET surface area, particle sizes, mean crystallite size, and unit-cell parameters from XRD study on powders calcined at 600 °C.

Sample	LSFC05 calcined at 600 °C
BET surface area ( $\text{m}^2/\text{g}$ )	21
Particle size $\phi_{10\%}$ ( $\mu\text{m}$ )	5.0
Particle size $\phi_{50\%}$ ( $\mu\text{m}$ )	11.6
Particle size $\phi_{90\%}$ ( $\mu\text{m}$ )	19.5
Mean crystallite size from XRD (nm)	24.5
$a$ ( $\text{\AA}$ )	5.5216(8)
$b$ ( $\text{\AA}$ )	7.816(1)
$c$ ( $\text{\AA}$ )	5.5520(8)
$V(\text{\AA}^3)$	239.62(6)

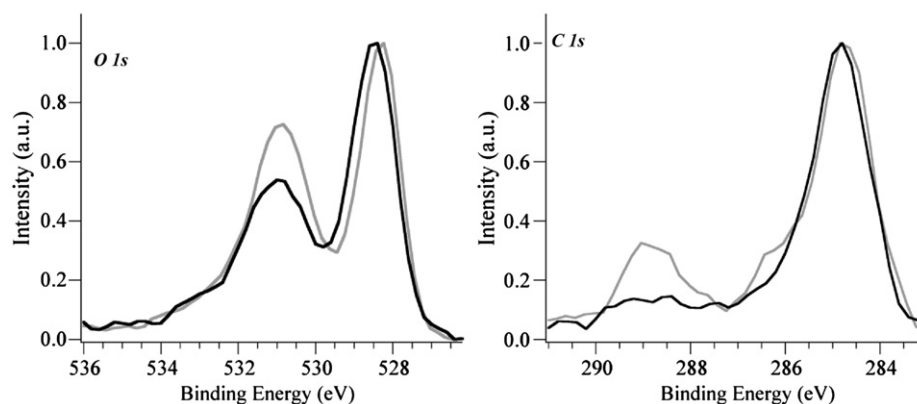


Fig. 2. O 1s and C 1s XP peaks obtained at room temperature for LSFC05 powder samples. LSFC05 sample aged 1 year (gray line), and aged 1 year and then heated at 900 °C for 1 h (black line). All spectra are normalized with respect to their maximum value.

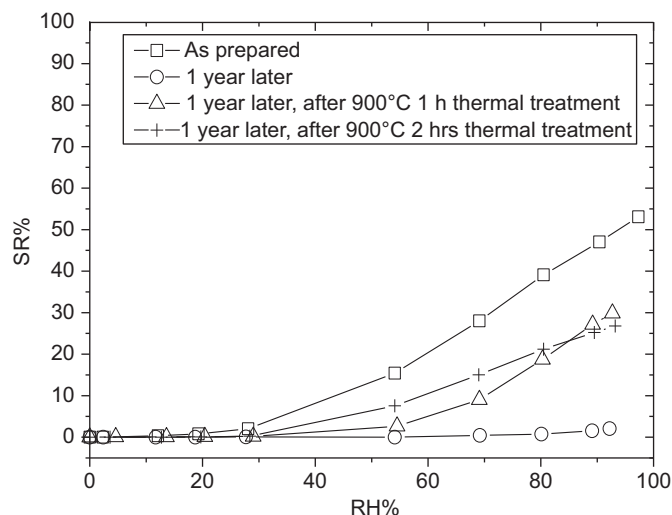


Fig. 3. Sensor response for LSFC05 as a function of relative humidity at different ageing times.

to two surface hydroxyls, and a proton may be transferred from a La(Sr)-OH group to a water molecule to form  $\text{H}_3\text{O}^+$  [9]. When more water vapor is adsorbed, more water molecules will cluster to form a liquid-like multilayer of hydrogen-bonded water molecules. Finally, these physisorbed water molecules condense into pores with size in the mesopore range (1–250 nm). Since the formation of clusters of  $\text{H}_2\text{O}$  and the hydration of  $\text{H}^+$  into  $\text{H}_3\text{O}^+$  are energetically favored in liquid water, the dominant charge carriers in the water adsorbed in the mesopores are  $\text{H}^+$ . The amount of  $\text{H}^+$  increases when increasing the moisture content, so  $\text{H}^+$  can move freely in liquid water, giving a decrease of grain surface resistance with increasing RH. This mechanism explains why  $R_g$ , defined in Eq. (1), tends to decrease with increasing RH, leading to an increase of SR, evidenced by all the sensors, though LSF is a known  $p$ -type semiconductor [9,10].

The rapid formation of phases of variable composition  $\text{La}_2(\text{CO}_3)_x(\text{OH})_{2(3-x)}$  has been already reported when lanthana was in contact with  $\text{CO}_2$  in humid environments. In perovskite-type  $\text{LaFeO}_3$  oxide, partially uncoordinated oxide ions are available to react with  $\text{CO}_2$ , producing stable surface carbonates [11]. Its formation could explain why humidity enhances the response of La doped tin oxide  $\text{CO}_2$  gas sensor [12]. Moreover, when these carbonates are insoluble in water, the sensing materials surface becomes hydrophobic, thereby reducing the interference from humidity, as reported for  $\text{BaCO}_3\text{--Li}_2\text{CO}_3$  electrodes [13].

#### 4. Conclusions

Physical–chemical analysis of the LSFC05 powders showed that (i) pure phase LSFC05 can be prepared by citrate auto-combustion method as shown by XRD, (ii) the morphology of the powders showed the presence of micrometric agglomerates (particle size) constituted of

nanosized primary particles, (iii) the BET surface area was  $21 \text{ m}^2/\text{g}$  and crystallite size of about 25 nm, and (iv) 5 mol% Cu-doping caused a moderate increment of the BET surface area. The XPS and IR measurements showed the presence of surface of hydroxide and carbonates species. After calcination at  $900^\circ\text{C}$  the amount of carbonates decreased but was still significant.

The sensing activity tests as a function of relative humidity at different ageing times were carried out for the first time. The results indicated that (i) after 1 year of ambient storage the sensing material lost quite completely its sensitivity to humidity, (ii) the sensing activity of the film was mostly re-activated after a thermal treatment at  $900^\circ\text{C}$  for 2 h, and (iii) the important shift of the detection limit to low RH caused by the presence of 5 mol% Cu is also restored. Further work will be required to investigate the chemical nature of metal carbonates and carbonate ions, and to ascertain the presence of oxide segregation at the surface.

#### Acknowledgments

The initial part of the work has been supported by INSTM and Regione Lombardia under the frame of the project “Nanostructured catalysts for energy and environment”.

#### References

- [1] A. Cavaliere, T. Caronna, I. Natali Sora, J.M. Tulliani, Electrical characterization of room temperature humidity sensors in  $\text{La}_{0.8}\text{Sr}_{0.2}\text{Fe}_{1-x}\text{Cu}_x\text{O}_3$  ( $x=0, 0.05, 0.10$ ), *Ceramics International* 38 (2012) 2865–2872.
- [2] I.N. Sora, T. Caronna, F. Fontana, C.D. Fernandez, A. Caneschi, M. Green, Crystal structures and magnetic properties of strontium and copper doped lanthanum ferrites, *Journal of Solid State Chemistry* 191 (2012) 33–39.
- [3] T. Caronna, F. Fontana, I. Natali Sora, R. Pelosato, Chemical synthesis and structural characterization of the substitution compound  $\text{LaFe}_{1-x}\text{Cu}_x\text{O}_3$  ( $x=0\text{--}0.40$ ), *Materials Chemistry and Physics* 116 (2009) 645–648.
- [4] R. Pelosato, C. Cristiani, G. Dotelli, M. Mariani, A. Donazzi, I. Natali Sora, Co-precipitation synthesis of SOFC electrode materials, *International Journal of Hydrogen Energy*, in press.
- [5] P.A.W. van der Heide, Systematic x-ray photoelectron spectroscopic study of  $\text{La}_{1-x}\text{Sr}_x$ -based perovskite-type oxides, *Surface and Interface Analysis* 33 (2002) 414–425.
- [6] M.M. Natile, F. Poletto, A. Galenda, A. Glisenti, T. Montini, L. De Rogatis, P. Fornasiero,  $\text{La}_{0.6}\text{Sr}_{0.4}\text{Co}_{1-y}\text{Fe}_y\text{O}_{3-\delta}$  perovskites: influence of the Co/Fe atomic ratio on properties and catalytic activity toward alcohol steam-reforming, *Chemistry of Materials* 20 (2008) 2314–2327.
- [7] G. Busca, V. Lorenzelli, Infrared spectroscopic identification of species arising from reactive adsorption of carbon oxides on metal oxide surfaces, *Journal of Materials Chemistry* 7 (1982) 89–126.
- [8] J.S. Feng, T. Liu, Y.B. Xu, J.Y. Zhao, Y.Y. He, Effects of PVA content on the synthesis of  $\text{LaFeO}_3$  via sol–gel route, *Ceramics International* 37 (2011) 1203–1207.
- [9] Z. Jing-Li, L. Yue-Dong, W. Guo-Biao, L. Biao-Rong, Electrical conduction of  $\text{La}_{1-x}\text{Sr}_x\text{FeO}_3$ , ceramics under different relative humidities, *Sensors and Actuators A: Physical* 29 (1991) 43–47.

- [10] M. Viviani, M.T. Buscaglia, V. Buscaglia, M. Leoni, P. Nanni, Barium perovskites as humidity sensing materials, *Journal of the European Ceramic Society* 21 (2001) 1981–1984.
- [11] M. Daturi, G. Busca, G., R.J. Willey, Surface and structure characterization of some perovskite-type powders to be used as combustion catalysis, *Chemistry of Materials* 7 (1995) 2115–2126.
- [12] A. Marsal, A. Cornet, J.R. Morante, Study of the CO and humidity interference in La doped tin oxide CO<sub>2</sub> gas sensor, *Sensors and Actuators B: Chemical* 94 (2003) 324–329.
- [13] I. Lee, S.A. Akbar, P.K. Dutta, High temperature potentiometric carbon dioxide sensor with minimal interference to humidity, *Sensors and Actuators B: Chemical* 142 (2009) 337–341.